ELSEVIER

Journal of Neuroscience Methods 115 (2002) 13–27

JOURNAL OF NEUROSCIENCE METHODS

www.elsevier.com/locate/jneumeth

Voltage-sensitive dye imaging of population neuronal activity in cortical tissue

Wenjun Jin [a,b], Ren-Ji Zhang [b], Jian-young Wu [a,*]

[a] *Department of Physiology and Biophysics, Georgetown University Medical Center, The Research Building, WP-26, 3900 Reservoir Road NW, Washington, DC 20007, USA*

[b] *Department of Physiology and Biophysics, Life Science College, Peking University, Beijing 100871, People's Republic of China*

Received 16 August 2001; received in revised form 16 November 2001; accepted 16 November 2001

Abstract

Voltage-sensitive dyes (VSDs) and optical imaging are useful for studying spatiotemporal patterns of population neuronal activity in cortical tissue. Using a photodiode array and absorption dyes we were able to detect neuronal activity in single trials before it could be detected by local field potential (LFP) recordings. Simultaneous electrical and optical recordings from the same tissue also showed that VSD and LFP signals have different waveforms during different activities, suggesting that they are sensitive to different aspects of the synchronization across the population. Noise, dye bleaching, phototoxicity and optical filter selection are important to the quality of the VSD signal and are discussed in this report. With optimized signal-to-noise ratio (S/N) and total recording time, we can optically monitor approximately 500 locations in an area of 1 mm^2 of cortical tissue with a sensitivity comparable to that of LFP electrodes. The total recording time and S/N of fluorescence and absorption dyes are also compared. At S/N of 8–10, absorption dye NK3630 allows a total recording time of 15–30 min, which can be divided into hundreds of 4–8 s recording trials over several hours, long enough for many kinds of experiments. In conclusion, the VSD method provides a reliable way for examining neuronal activity and pharmacological properties of synapses in brain slices.

Keywords: Optical recordings; Brain slice; Rat; Somatosensory cortex; Auditory cortex; Amygdaloid; Diode array; CCD camera

1. Introduction

Voltage-sensitive dye (VSD) imaging, an optical method of measuring transmembrane potential, has been undergoing development since the pioneering work published about 30 years ago (Cohen et al., 1968; Tasaki et al., 1968). With better dyes and specialized apparatus, the method has gradually evolved from technological demonstrations into a practical tool for imaging the activity of excitable tissues.

After screening thousands of compounds (Gupta et al., 1981; Grinvald et al., 1982a; Loew et al., 1992; Shoham et al., 1999), a dozen were found useful, and a number of them became commercially available. These dyes have very fast response times (< 1 us) and excellent linearity (± 300 mV, Ross et al., 1977), but all have small fractional changes in absorption or fluorescence. In biological tissues the fractional changes are only about 10^{-2}–10^{-5} of the resting light intensity (RLI) per 100 mV of membrane potential change.

In the past 10 years or so, new dyes based on fluorescence resonance energy transfer (FRET) have been developed which have the potential to yield much larger signals ($\sim 10^{0}$–10^{1}) (Cacciatore et al., 1999). However, these dyes are still too slow to follow action potentials (Taylor et al., 2000) and the methods for loading dyes into biological tissue need to be improved before they can be used for most of the applications.

Before the new FRET dyes become available, all VSD measurements are forced to use the old dyes with small fractional changes. However, a small fractional change does not always imply a poor signal-to-noise ratio. In this report we show that in brain slice preparations it is possible to reduce noise and achieve a decent signal-to-noise ratio (5–30) in single recording trials.

* Corresponding author. Tel.: +1-202-687-1617; fax: +1-202-687-0617.

E-mail address: wuj@georgetown.edu (J.-y. Wu).

0165-0270/02/$ - see front matter
PII: S0165-0270(01)00511-8

This signal-to-noise ratio would allow imaging of the initiation and propagation of population activity without averaging, which is particularly useful for examining the dynamics of population neuronal activities.

Cortical tissue is rich in neuropils and thus has a relatively large area of stained excitable membranes per unit volume. During population events cortical neurons are usually activated in ensembles; the combined dye signals from many neurons may be significantly larger. These factors make cortical tissue a preferred preparation for VSD measurements.

Imaging with VSDs not only provides information about where the activity occurs and how it propagates, but also about the synchrony of the activity, i.e. the fraction of neurons activated in a population in a given time bin.

Over the last 20 years many authors have published VSD imaging studies using brain slices (Grinvald et al., 1982b; Albowitz and Kuhnt, 1993; Colom and Saggau, 1994; Tanifuji et al., 1994; Hirota et al., 1995; Tsau et al., 1998a, 1999; Demir et al., 1999, 2000; Laaris et al., 2000; Wu et al., 1999b, 2001, for reviews see Ebner and Chen, 1995; Wu et al., 1999a), but most of the works concentrated on the scientific subject without discussing technical details for measuring small VSD signals. Two recent papers by Momose-Sato et al. (1999), Tominaga et al. (2000) have described dyes and methods for detecting larger (10^{-3}–10^{-2}) and averageable signals in hippocampal slices. There is an increasing interest in detecting small (10^{-5}–10^{-4}) VSD signals in cortical tissue during oscillations and other population activities (Wu et al., 1999b, 2001). These signals are not synchronized to the stimulus and cannot be averaged. In this report we will discuss the optimized methods for detecting such small signals in single trials.

2. Methods

2.1. Preparation of cortical slices

Sprague–Dawley rats of both sexes from P14 to P35 were used in the experiments. Following NIH guidelines, the animals were deeply anesthetized with halothane and quickly decapitated using a Stoelting small animal decapitator. The whole brain was chilled in cold (0–4 °C) artificial CSF [ACSF, containing (in mM) NaCl, 132; KCl, 3; $CaCl_2$, 2; $MgSO_4$, 2; NaH_2PO_4, 1.25; $NaHCO_3$, 26; dextrose 10; and saturated with 95% O_2, 5% CO_2] for 90 s before slicing. Coronal slices (400 um thick) from somatosensory and auditory cortices were cut with a vibratome stage (752M Vibroslice, Campden Instruments, Sarasota, FL) and transferred to a holding chamber where the solution was slowly bubbled by a mixture of 95% O_2 and 5% CO_2. Slices were incubated for at least 1 h before the experiment.

2.2. Staining with voltage-sensitive dye

The staining chamber contained about 50 ml of ACSF, bubbled with O_2–CO_2 gas and circulated by a stirring bar. For absorption measurements the slices were stained with 0.005–0.02 mg/ml of an oxonol dye, NK3630 (first synthesized by R. Hildesheim and A. Grinvald as RH482; available from Nippon Kankoh-Shikiso Kenkyusho Co., Ltd., Japan), for 30–60 min. For fluorescence measurements the slices were stained with 0.01–0.05 mg/ml of fluorescent dye, RH 795 (first synthesized by R. Hildesheim and A. Grinvald; available from Molecular Probes), for 45–60 min. After staining the slices were transferred back to the holding chamber (to rinse out excess dye) and held in the chamber until needed in the experiments.

2.3. Optical imaging apparatus and light intensity

VSD imaging was performed with a 124-element photodiode array (Centronics Inc., Newbury Park, CA) at a frame rate of 1000 frames per s. The array was mounted on the 'C' mount of a fixed-stage microscope (Zeiss Axiophot). Objectives of 5× (0.12 NA, Zeiss), 20× (0.6 NA, water immersion, Nikon) or 40× (0.75 NA, water immersion, Zeiss) were used to project the image of the preparation onto the array. Each photodetector received light from an area of 0.33×0.33, 0.08×0.08, and 0.04×0.04 mm^2 of tissue for the 5×, 20× and 40× objectives, respectively. The light source for the optical recording was a 100 W halogen–tungsten filament bulb. We use the term 'illumination intensity' to describe the light intensity that the tissue receives during the imaging and RLI for the light intensity reaching the diode array. Usually the RLI is about 1/100 to 1/10 000 of illumination intensity during absorption and fluorescence measurements. In our experiments the RLI was about 10^9 photons per ms per detector for absorption dyes and about 10^7 photons per ms per detector for fluorescence measurement. The photocurrent from each photodetector was individually amplified through a two-stage amplifier system. The first stage performed a current-to-voltage conversion. In our array the RLI was converted to a voltage of about 5 V. This voltage is also referred to as RLI in this report.

The VSD signal is a fractional change (0.001–0.1%) on a large DC component. When the RLI is ~5 V, the full range of the signal is only about 0.05–5 mV. A DC subtraction/high-pass filter (1000 ms time constant or 0.16 Hz corner frequency) circuit was used for each individual detector to eliminate the DC component (the entire RLI). The signal (dye related fractional changes) was then amplified 200–1000 times. This allowed the small fractional change (e.g. 10^{-4}) to be digitized in the full range of 12 bits. Before digitizing, a four-pole

Bessel analog low-pass filter with a 333 Hz corner frequency was applied to ensure that the frequency of the analog signal was lower than the Nyquest frequency of the sampling. Signals were multiplexed and then digitized with a 12-bit data acquisition board (Microstar Laboratories, Bellevue, WA) installed in a computer (Pentium PC).

A commercial diode array system with similar performance and higher spatial resolution (464 photo elements and eight electrical channels) is available from WuTech Instruments, Gaithersburg, MD (www.wutech.com) as the 469III diode array system or the NEUROPLEX II package (together with NEUROPLEX software) from RedShirtImaging, LLC, Fairfield, CT (www.RedShirtImaging.com). Additional details about the diode array circuits and noise consideration were discussed in Wu and Cohen (1993) and Wu et al. (1999a).

2.4. Local field potential recordings

Tungsten lacquer-coated microelectrodes (FHC, Bowdoinham, ME) were used to simultaneously sample local field potentials (LFP). The tip resistance of the electrodes ranged from 75 to 200 K-ohm. In order to minimize the damage to the cortical tissue the electrodes were carefully inserted about 100 μm into the slice in cortical layers II–III. With careful placement of the LFP electrode the tissue surrounding it produced normal VSD signals, which is important for comparing electrical and optical signals. Electrical recordings were digitized and stored concurrently with the optical images. The LFP signals were amplified 1000× and bandpass filtered at 0.1–400 Hz (by a Brownlee Precision 440 amplifier) and digitized concurrently with VSD signals.

2.5. Vibration isolation

During absorption measurements photodetectors receive high intensity light and, therefore, are extremely sensitive to vibration noise. A standard air table is usually not sufficient for isolating the floor noise. We found that the 'Minus K' isolation stage (www.minusk.com) is excellent in isolating low frequency floor vibrations. At 5 Hz the amplitude of the vibration on this table was about 1/10 of that on an air table from Newport. Vibration noise will be discussed in Section 3.3.

2.6. Data analysis and display

The optical data were analyzed using the program NEUROPLEX (A. Cohen, C. Falk and L.B. Cohen, RedShirtImaging, LLC). Data were displayed in the form of traces for numerical analysis and pseudocolor images for visualizing the spatiotemporal patterns. An example of data display is illustrated in Fig. 1, where the waveforms from the LFP electrode and one optical detector viewing the same location are shown in Fig. 1A. In Fig. 1C the spatiotemporal pattern of the activity is presented by means of pseudocolor maps (Senseman et al., 1999). To compose a pseudocolor map, signals from each individual detector are normalized to their own maximum amplitude (peak = 1 and baseline/negative peak = 0). Then a scale of 16 colors are linearly assigned to the values between 0 and 1. In this paper pseudocolor maps are displayed as 'contour' maps using the CONTOUR function provided by IDL (Interactive Display Language, Research Systems Inc., Boulder, CO) and used by NEUROPLEX.

In Fig. 1c only a few VSD images (1 ms snapshots) selected from a total of 2000 images (a 2 s recording trial at 1 frame per ms) are shown. The times of the images are marked as points a–f in Fig. 1A, with reference to the LFP signal. The interictal-like spike was initiated at the stimulation point in the deep layers and propagated vertically and then horizontally as a wave. In this example imaging the activity in a single trial (without averaging) is important, because the initiation and propagation of the activity varies significantly from trial to trial (Tsau et al., 1998a).

Throughout this paper the signal-to-noise ratio is defined as the amplitude of the VSD signal divided by the root mean square (RMS) value of the baseline noise.

3. Results and discussion

3.1. Comparison of dye signals and local field potential

Although LFP and VSD recordings, both monitor the neuronal population activity, the sources of the signals are different. The amplitude of LFP signal is proportional to the current density near the tip of the electrode while VSD measures the transmembrane potential. Thus the waveforms of the two measurements from the same cortical tissue may be significantly different during some activities.

3.1.1. Waveform

When a single neuron was simultaneously measured by VSD imaging and an intracellular electrode, the waveforms of the two recordings were remarkably similar (Ross et al., 1977; Zecevic, 1996; Fig. 2A). However, this remarkable similarity only occurs when a single neuron is measured intracellularly. During population activities the VSD waveform follows the sum of the transmembrane potential of all stained membranes under one detector, and thus may be very different from either the individual neuron's intracellular poten-

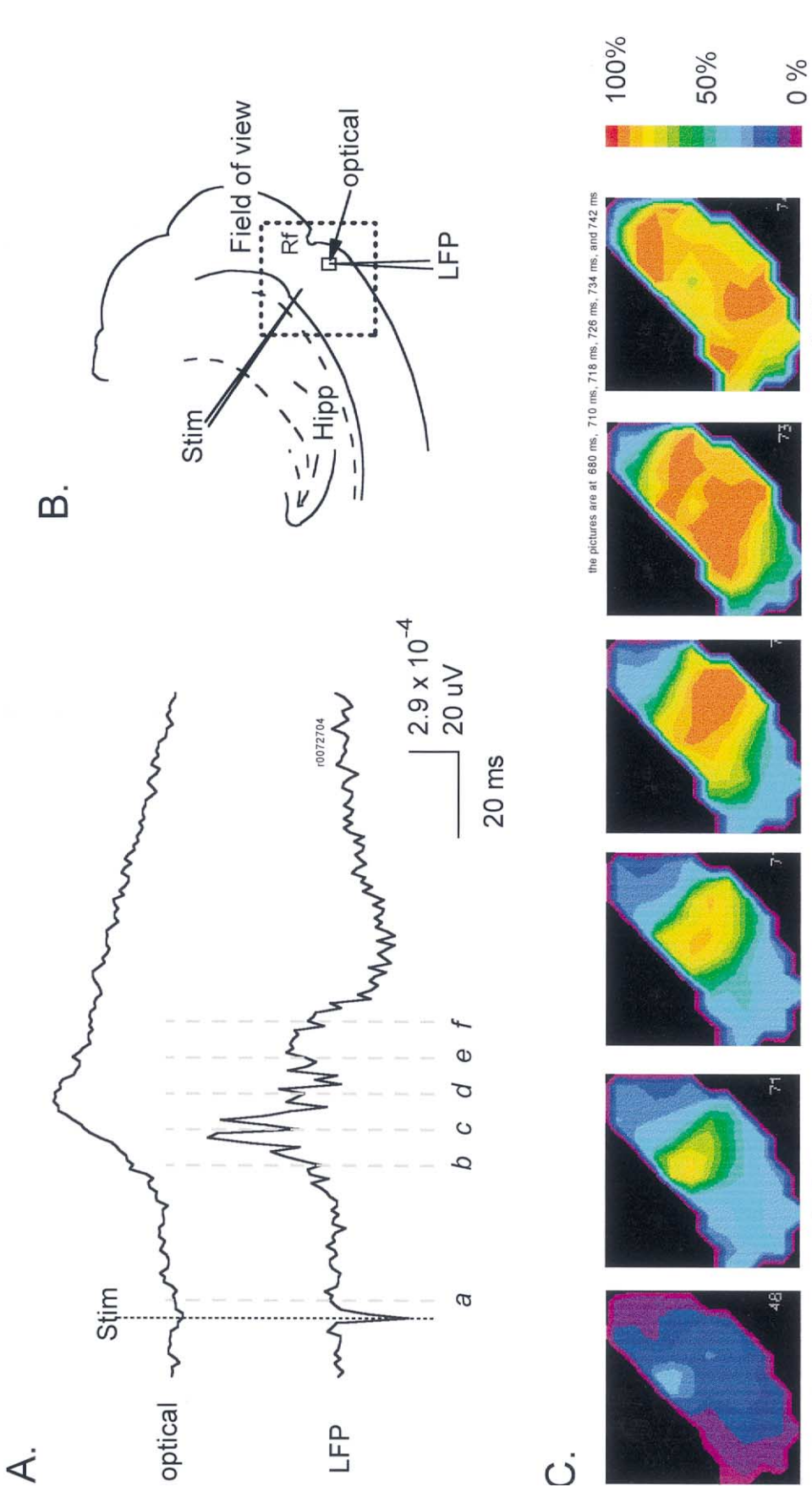

Fig. 1. An example of displaying VSD data. (A) Trace display. VSD signals are displayed in comparison with a simultaneous electrical recording (LFP) from the same location (cortical layer II–III) during an evoked interictal-like spike. The preparation was a coronal slice stained with NK3630, and perfused with 1 μM bicuculline. Both traces are unfiltered data of a single trial. (B) Location map. The relative locations of preparation, field of view and the stimulation-recording arrangement are sketched. Stim, stimulation electrode; LFP, local field recording electrode. The small square around the LFP electrode is the location of the optical detector whose signal is shown in A. Hipp, hippocampus; Rf, Rhinal Fissure. (C) Pseudocolor images. This kind of display shows the spatiotemporal distribution of the population activity. In this example six snapshot (1 ms) images were selected from 2000 images. The snapshots were taken at the times labeled as *a* through *f* in A.

tial recording or the LFP recorded at the position of the optical detector. When a large portion of the neurons in the tissue are stained with VSD ('massive staining' as in this report), signals of individual neuron spikes are buried in the shot noise (which comes from the light from other stained tissue and neurons that are not contributing to the signal and, in absorption, from light that does not interact with dye) and become invisible without averaging (explained in detail by Cohen and Lesher, 1986). Individual neuron spikes in brain slices are only visible when just one neuron is stained by intracellular dye injection (Antic et al., 1999).

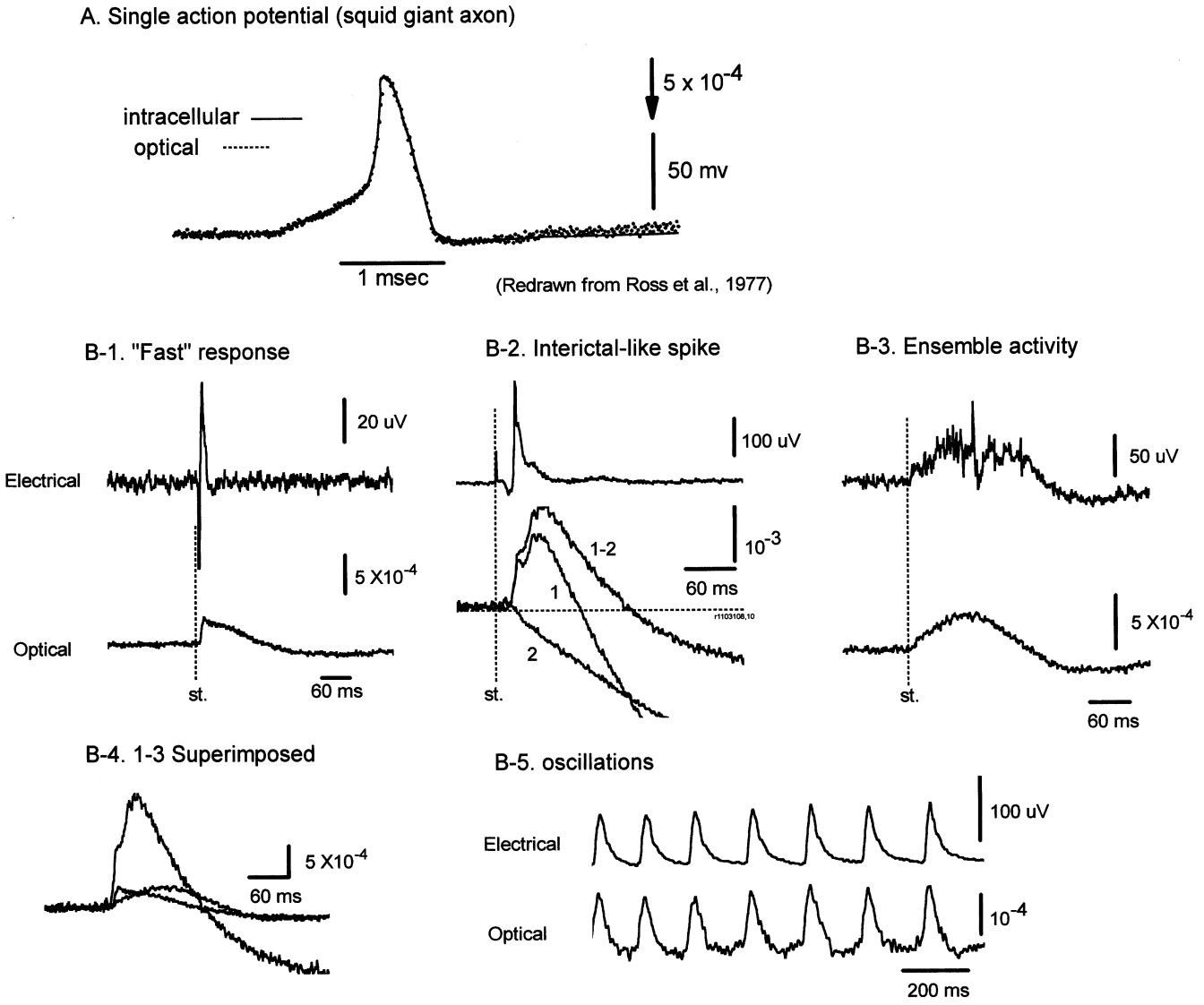

Fig. 2. Comparison of optical and electrical recordings. (A) VSD and intracellular recordings during a single action potential. The change in absorption at 705 nm (dotted trace) was recorded from a squid giant axon stained by a voltage-sensitive dye XVII. The actual membrane potential change (smooth trace) was simultaneously recorded by an intracellular electrode. The time course of the VSD signal matched accurately to that of the membrane potential change. Note that the amplitude of the VSD signal is very small (Redrawn from Ross et al., 1977). (B) LFP (top traces) and VSD (bottom traces) recordings during different kinds of population activities. The recordings were simultaneously made from the same location in cortex layer II–III of rat somatosensory cortical slices. (B-1) A short latency activity (fast response) was evoked by an electrical shock to the white matter; the slice was bathed in normal ACSF. (B-2) An evoked interictal spike (Tsau et al., 1999); the slice was bathed in 10 μM bicuculline. During this activity a large fraction of neurons was activated and changes in light scattering also contributed to the signal. Here trace 1 is the light intensity change at 705 nm; trace 2 is the intensity change at 520 nm, presumably the light scattering signal; subtraction of the signal at the two wavelengths (trace 1–2) is likely the VSD signal without the contamination of light scattering. (B-3) An evoked polysynaptic event ('ensemble activity', Wu et al., 2001). Note that in B-1 and B-2 the duration of VSD signals was longer than that of LFP; however, in B-3 the durations were similar but the LFP signals contained high frequency fluctuations. (B-4) VSD traces of B-1, B-2 (trace 1–2), and B-3 were superimposed, showing the difference in amplitude and time course. (B-5) A spontaneous 7–10 Hz oscillation (Wu et al., 1999b) in which LFP and VSD signals were well correlated.

Fig. 2B compares the waveforms of LFP (top traces) and VSD (bottom traces) recordings during four different forms of population activity. Fig. 2B-1 shows a short latency ('Fast') response to an electrical stimulus to the white matter (slice bathed in normal ACSF). This response had a short latency and the amplitude of VSD signal was proportional to the stimulus intensity. Presumably the response was mainly contributed by neurons activated either directly by the stimulus or via a few synapses. The LFP response had a short duration (< 30 ms) but the VSD signal from the tissue surrounding the electrode had a much longer duration. This long optical signal did not appear at 520 nm, indicating that it was a wavelength dependent VSD signal, instead of a wavelength independent signal resulting from light scattering or other intrinsic signals (Pazdalski et al., 1998). The long duration of the VSD signals suggests that after the initial phase of the fast response there was an asynchronized firing period which was not detectable by the LFP, probably because during the asynchronized spiking period depolarizing and repolarizing currents canceled each other out or because current flows may be briefer than the potential elevation. Dye molecules bound to the glial cells may also contribute to this long period due to glial membrane potential change caused by glutamate transporters (Kojima et al., 1999; Momose-Sato et al., 1999).

Fig. 2B-2 shows optical and electrical signals from an interictal-like spike (slice bathed in 10 uM bicuculline) evoked by a weak electrical shock to the white matter, measured in cortical layers II–III. Interictal-like spikes are all-or-none population events; the amplitude of the dye signal is relatively large and independent from the stimulus intensity. Again VSD signals had a long duration with a smooth waveform while LFP signals had a short duration and large fluctuations. VSD signal during an interictal-like spike had an obvious undershoot (move downward below the baseline after the positive peak). Part of this undershoot also occurred at 520 nm (Fig. 2B-2, trace I), suggesting that it was caused by light scattering signal. The sign of the light scattering signal under trans-illumination was opposite that of the VSD signal of NK3630 at 705 nm. Light scattering also had a slow onset (a tau of ~ 100 ms) and the amplitude was linearly proportional to the portion of the neurons being activated (Pazdalski et al., 1998).

Fig. 2B-3 shows another evoked population activity, 'ensemble activity' (slice bathed in normal ACSF, Wu et al., 2001). This activity is also an all-or-none population event but the VSD signal amplitude is only about 1/10–1/4 of that of the interictal-like spikes (Fig. 2B-2). This indicates that this activity contains a much lower density of active neurons than do interictal-like spikes. Interestingly, during this activity the duration of VSD and LFP signals were similar. However, LFP signals contained complex fluctuations (Wu et al., 2001) while VSD signals had a smooth waveform.

In Fig. 2B-4 the waveform of VSD signals during the three population events shown in Fig. 2B1-3 are plotted in superimposed traces, illustrating the differences in amplitude and time course. If the neurons are evenly stained, the amplitude of the VSD signal should be linear to the synchrony of the activity and the area under the waveform envelope should be linear to the number of total spikes during the event. Fig. 2B-4 suggests that the synchrony and duration during different cortical events are two independent variables. Higher synchrony (larger portion of neurons depolarize in each time bin) is not always accompanied by longer duration.

Fig. 2B-5 shows another example of VSD-LFP waveforms of a population event. During a spontaneous oscillation (cortical slice bathed in low Mg media)—VSD and LFP signals had very similar waveforms and similar frequency compositions (Wu et al., 1999b).

These comparisons suggest that the difference between VSD and LFP waveforms is related to the nature of the population activity in the cortical neural network. The VSD signals are linearly correlated to the potential changes of all the membranes under one detector. LFP signals, on the other hand, are a non-linear summation of the current sources distributed around the tip of the electrode. LFP amplitude decreases with the square of the distance between the source and the electrode. Thus, in this situation the LFP signal is likely to report localized activity surrounding its tip, although LFP recordings can also be sensitive to the strong current flow far away from the electrode.

3.1.2. Sensitivity

Sensitivity of VSD measurement is important for detecting small population activities. Here the detecting ability of VSD measurements was compared with that of a LFP electrode from the same tissue (Fig. 3).

A neocortical slice (rat barrel cortex) was stained by NK3630 and cortical layer II–III was monitored optically. A LFP electrode was placed in the tissue at the same location as the optical measurement. Electrical stimulation was delivered to the deep layers of the cortex and evoked a 'fast' response. In one slice, when the stimulus intensity was about 12% of the intensity that generated maximum VSD signal (the saturation intensity), the fast response was seen in both LFP and VSD recordings (Fig. 3A). When the stimulus intensity was reduced to 9% of the saturation intensity, the response on the LFP could not be detected (below 'threshold'), but the VSD trace still showed a reliable response in every single trial (Fig. 3B). In cortical tissue the main power of the VSD signal was below 50 Hz in all four population events we have examined (Fig. 2B). Thus a proper low-pass filter could further improve the signal-to-noise ratio. The bottom traces in Fig. 3A and

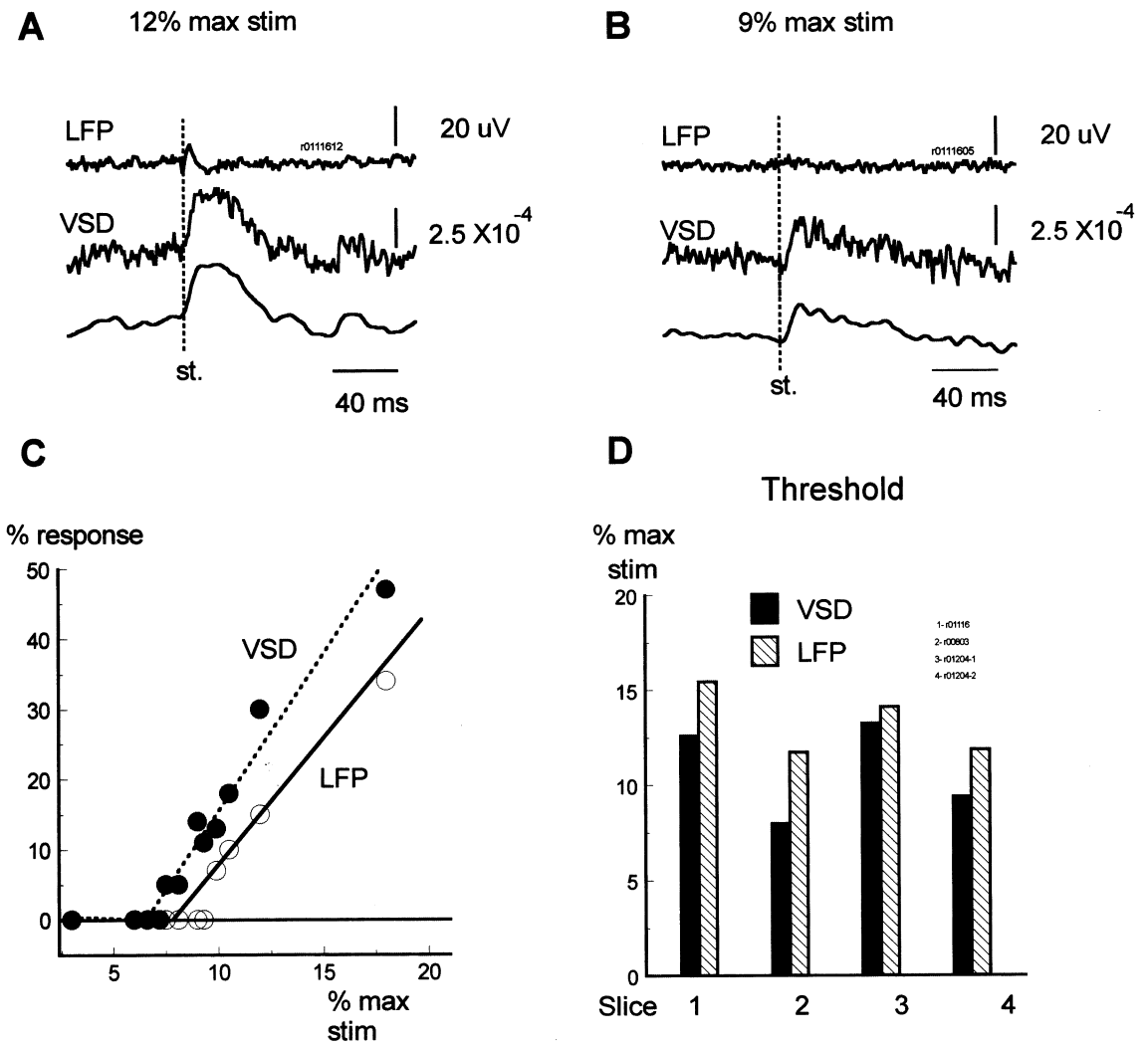

Fig. 3. Sensitivity of VSD and LFP measurements. VSD and LFP signals during the fast response were recorded from the same location in layer II–III. (A) At 12% of the stimulation intensity which generated a maximum response, the fast response was visible in both LFP and VSD signals. (B) With the stimulus reduced to 9% of the maximum intensity, only VSD response was visible. The bottom trace of panels A and B are the VSD signal filtered at 50 Hz, showing an improved signal-to-noise ratio. (C) A stimulus–response curve showing that VSD measurement is more sensitive than LFP recordings from the same tissue. (D) In four different slices VSD measurements always had higher sensitivity than the LFP electrode.

B are the same data as the middle traces but low-pass filtered at 50 Hz, resulting in an improved signal-to-noise ratio. This data suggests that VSD measurement in brain slice is more sensitive than the LFP in detecting small population activity.

Stimulus–response curves made with both sub- and super-threshold stimuli (Fig. 3C) further confirmed the sensitivity of VSD measurement. Fig. 3D shows the detecting threshold in four slices tested. Although the thresholds for VSD and LFP measurements were different in different slices, VSD measurement always had a higher detecting sensitivity than the LFP electrode.

Using objectives with larger optical magnification reduces the volume of tissue covered by each photodetector. When a 40 × objective was used, each photodetector was measuring $40 \times 40\ \mu m^2$ of cortical tissue, and the signal-to-noise ratio was reduced to about 60% of that obtained when using a 5 × objective (Fig. 4). A comparison of the data in Figs. 3 and 4 suggests that even with a high spatial resolution (40 × magnification) the sensitivity of the optical measurement would still be comparable to that of LFP measurement.

The sensitivity comparison suggests that VSD imaging is useful for simultaneously measuring hundreds of locations on a brain slice to examine the initiation and propagation of population activities. Data in Figs. 3 and 4 indicate that it is practical to record ~500 locations in an area of ~1 mm in diameter ($40 \times 40\ \mu m^2$ per detector), with a sensitivity similar to that of a LFP electrode.

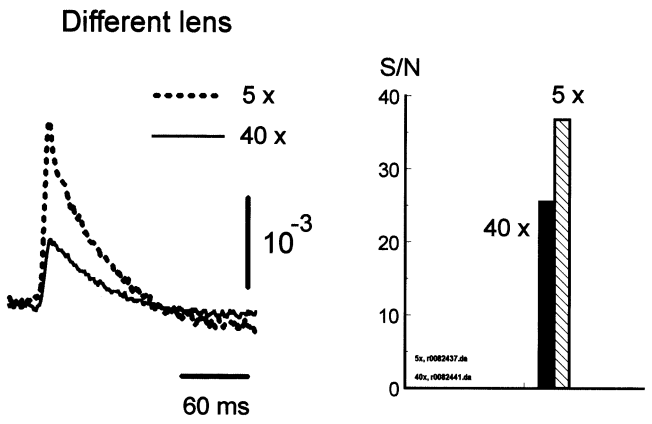

Fig. 4. Comparison of different optical magnifications. Left: VSD signals under a $5\times/0.12$ NA objective (dotted line) and a $40\times/0.7$ NA water immersion objective. The tissues covered under the two objectives were 330×330 and 41×41 μm^2, respectively. (B) Signal-to-noise ratio of the fast response evoked by the same stimulus intensity measured from the same cortical tissue.

3.2. Resting light intensity

Several kinds of noise in VSD measurements are related to the RLI. In an ideal situation the signal-to-noise ratio should be limited only by shot noise (the statistical fluctuation of the photon flow). Since the amplitude of the VSD signal is proportional to the RLI and the shot noise is proportional to the square root of the RLI, signal-to-noise ratio is thus proportional to the square root of the RLI (Cohen and Lesher, 1986); working in a high light level can thus increase the sensitivity of the measurement. In addition instrument noise of the imaging system (dark noise) becomes insignificant at a high RLI when shot noise is dominant. However, many imaging devices (e.g. most CCD cameras) cannot work in a high light level. When working in a low RLI, the instrument noise may become a limiting factor of signal-to-noise ratio (e.g. in Shoham et al., 1999).

Fig. 5A shows signal-to-noise ratio of absorption measurements at four different resting light intensities. By changing the lamp current, illumination intensity was continuously adjustable and desired resting light intensities were obtained. At a low light intensity of $\sim 5.8\times10^8$ photons per ms per mm^2, the signal-to-noise ratio was poor; apparently the dark noise was dominant (Fig. 5A-a; the signal-to-noise ratio is defined as the amplitude of the signal divided by the RMS value of the baseline). The bottom traces in Fig. 5A-a are the same data filtered at 50 Hz; the signal was more noticeable but the signal-to-noise ratio was still only about 1:1 (averaging made it more noticeable, data not shown). In the other three panels of Fig. 5A, RLI was increased into the range of practical measurement; the measurements are all shot noise dominant. In Fig. 5B the signal-to-noise ratio (calculated at a bandwidth of 1–500 Hz) was plotted against four different resting light intensities. The dashed line is a theoretical square-root curve. This plot suggests that with a combination of diode array and absorption dyes, the measurement can be dominated by shot noise when the RLI is higher than 5×10^9 photons per ms per mm^2.

RLI cannot be increased without limitation. Due to phototoxicity and bleaching, RLI has to be limited to allow an acceptable total recording time (Section 3.4).

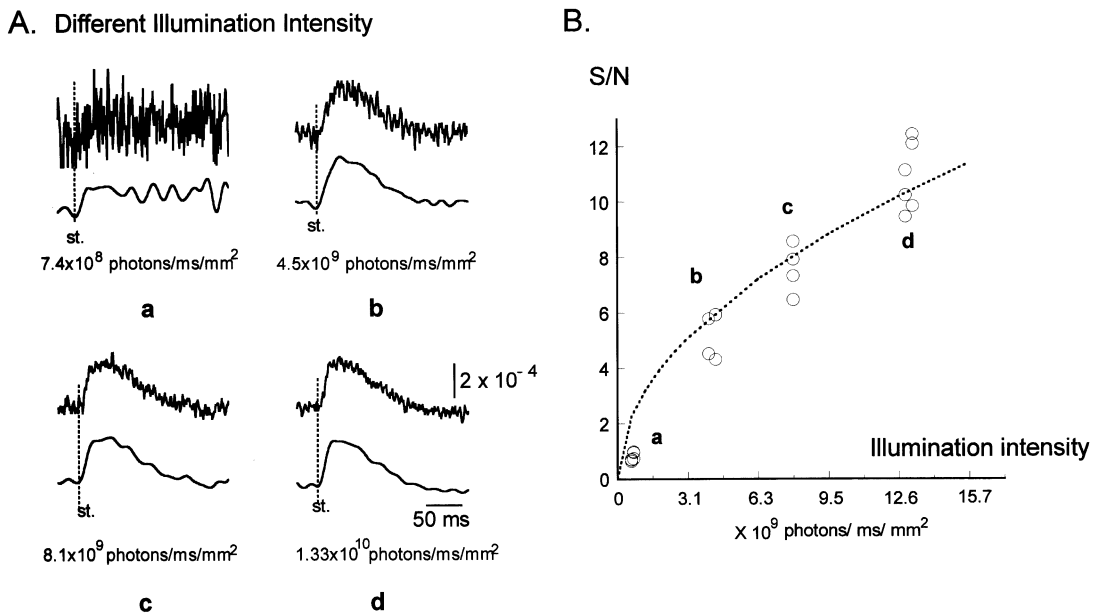

Fig. 5. Signal-to-noise ratio of absorption measurement at different resting light intensities. (A) All the traces represent the fast response measured from the same tissue (layer II–III, slice bathed in normal ACSF). In each panel the top traces were unfiltered VSD signals and the bottom traces were the same data filtered at 50 Hz. (B). Signal-to-noise ratio at the four different resting light intensities (filtered at 50 Hz).

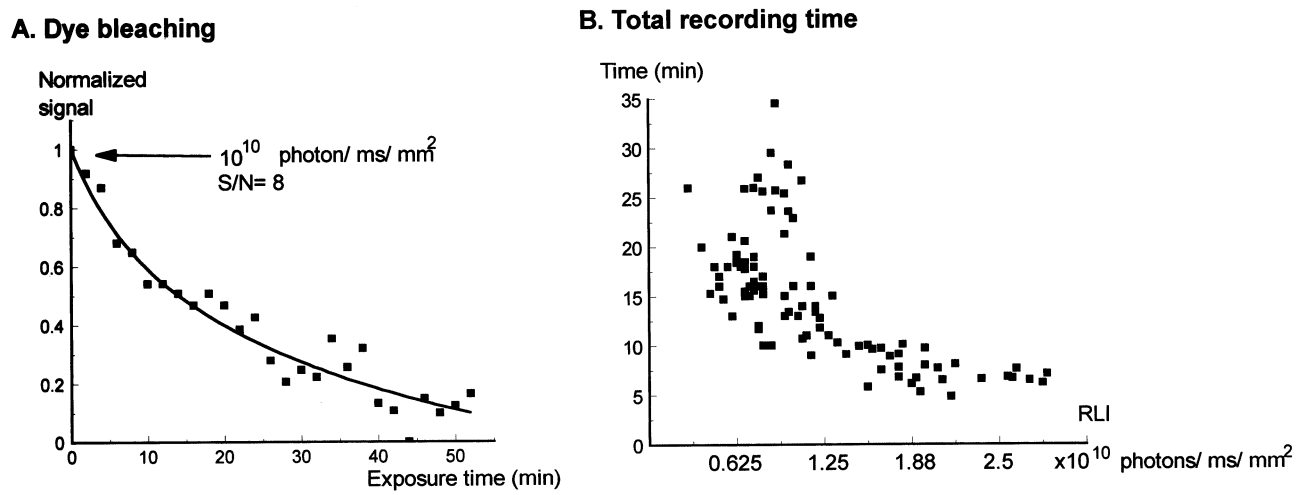

Fig. 6. Dye bleaching and total recording time. (A) Reduction of VSD signal due to light exposure. The slice was stained with NK3630 and exposed to an illumination intensity of 5×10^{11} photons per ms per mm^2 (RLI was $\sim 10^{10}$ photons per ms per mm^2).The exposures were 2 min trials with 2 min intermittent dark periods. The reduction of the optical signal was likely due to bleaching of the dye molecules on the membrane. (B) The total recording time was defined as the exposure time needed for the VSD signals to decrease to 50% of the pre-exposure amplitude. The plot was composed of data from ~ 25 locations in four slices.

3.3. Vibration noise

Vibration noise is defined as the light intensity changes on a photodetector caused by the movement of the image. Absorption measurement has small fractional changes and a high RLI on the detectors, so it is sensitive to the movement of the preparation.

Vibration noise is proportional to the RLI while shot noise is proportional to the square root of the light intensity. Thus when illumination intensity increases, vibration noise will ultimately become dominant. Above the level where vibration noise equals the shot noise, signal-to-noise ratio will no longer increase with higher illumination intensity. When high illumination intensity is used (e.g. absorption methods), vibration control in many situations determines the ultimate signal-to-noise ratio.

We use the following method for evaluating the vibration noise on a given apparatus:

Under Koehler illumination reduce the field diaphragm of the microscope so that a clear image of the diaphragm (as a round hole with a sharp edge) is formed in the field of view and project the image onto the photodetector. The sharp edge of the image generates a near maximum contrast on the imaging system. Due to the vibration, the edge may move in the image plane so that the light intensity on some detectors viewing the edge changes from minimum to maximum and on other detectors changes from maximum to minimum. The intensity change on the detectors will reflect the worst possible effect of vibration noise. When the experimental stage is well isolated, the noise on the edge of the hole should not be larger than that in the center of the hole. With the chamber and preparation inserted into the light path, the vibration noise may also become larger because of the vibration of the water air interface. A cover slip or water immersion lens can eliminate this kind of vibration noise.

With this test we found that air tables performed poorly in filtering vibrations below 5 Hz. A novel isolation stage designed for atomic force microscopy, the 'Minus K' table (www.minusk.com), is about ten times better than our air tables. With the Minus K table the vibration noise can be reduced below the level of shot noise at a RLI of $\sim 10^{11}$ photons per ms per mm^2.

3.4. Total recording time

Phototoxicity and dye bleaching set the limit for illumination intensity and total recording time. When stained slices were continuously exposed to high intensity light (e.g. $\sim 10^{12}$ photons per ms per mm^2), LFP signal and optical signal decreased gradually after 5–10 min. We define this reduction in electrical activity due to exposure as 'phototoxicity' (also called photodynamic damage, Cohen and Salzberg, 1978). Phototoxicity in cortical slices appeared to be irreversible even after a long dark recovery period.

Intermittent exposure significantly reduced phototoxicity. At an illumination intensity of 10^{12} photons per mm per mm^2 (RLI ~ 10 photons per mm per mm^2) when exposure is broken down to 2 min sessions with 2 min dark intervals, phototoxicity of NK3630 became less significant. In nine out of ten slices LFP signals dropped only $< 30\%$ after 60 min of total exposure time. Optical signals, however, dropped $\sim 90\%$ (Fig. 6A). We define 'bleaching' as the reduction in optical

signal while LFP signals remain unchanged. After long exposure the bleaching effect was visible as the exposed area lost color. Optical signals recovered in the bleached area after the preparation was restained (data not shown).

We define the total recording time as the exposure time needed to reduce the amplitude of the optical signal to 50% of the pre-exposure level. Fig. 6B shows the total recording time at different resting light intensities. Using Fig. 5B, Fig. 6B we know that when illumination intensity was adjusted for a signal-to-noise ratio of 8–10, the total recording time was about 15–30 min. This time can be divided into many intermittent recording sessions (e.g. 100 of 8 s trials). This total time appears to be enough for most experiments.

3.5. Wavelength and filter selection

Fig. 7A shows the absorption spectrum of unstained cortical tissue and the spectrum of tissue stained with dye NK3630. Unstained brain tissue has a relatively even transmission with a tendency to absorb less in longer wavelengths (Fig. 7A, open circles). Stained cortical tissue has a peak of absorption around 670 nm (Fig. 7A, solid circles). This peak stayed the same after a long wash with dye-free ACSF. For a satisfactory staining the light transmission at 670 nm (peak absorption) through a 400 μm stained slice was reduced to 1/10–1/50 of that of unstained slices.

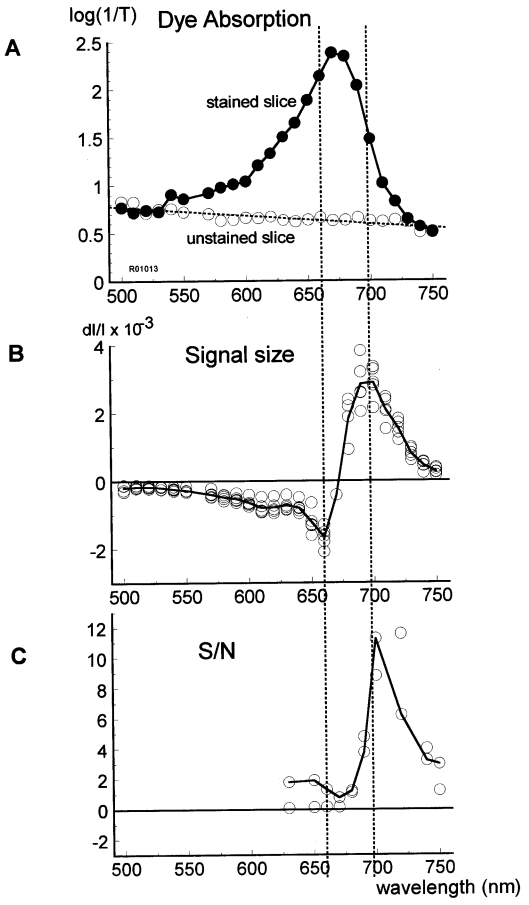

Fig. 7. Absorption spectra and signal-to-noise ratio. (A) The absorption spectrum of unstained slices (unfilled circles) and a slice stained with NK3630 (solid dots). (B) VSD signal amplitude at different wavelengths. Note that the maximum amplitude is not at the peak absorbance. (C) Signal-to-noise ratio at different wavelengths.

In Fig. 7B and C the amplitudes of the dye signal (dI/I) and signal-to-noise ratio are plotted against wavelength. The dI/I and signal-to-noise ratio reached a maximum at 705 nm. The signal decreased significantly at wavelengths shorter than 690 nm and reached a minimum at $\sim$675 nm. At wavelengths shorter than 670 nm the signal became larger but the polarity of the signal reversed. The signal reached a second maximum at 660 nm. After this 660 nm peak, the signal decreased gradually and became undetectable at wavelengths of 550 nm or shorter. This plot shows several useful wavelengths: For non-ratiometric measurement, band pass filtering around 705 nm should yield the largest signal; An alternating illumination of 700 and 660 nm may be used for ratiometric measurements; Illumination at 675 nm should provide a minimum VSD signal, which can be used for measuring light scattering or for distinguishing VSD from intrinsic signals.

The signal-to-noise ratio spectrum in Fig. 7C suggests that the best filter for NK3630 should have a center wavelength around 705 nm. The bandwidth of the filter, however, depends upon other factors: When the signal is small and shot noise is a limiting factor, a wider bandpass would allow more light and thus increase the signal-to-noise ratio. In this case the filter should have a center wavelength of 715 and a bandwidth of ± 30 nm. When measuring large signals, where long total recording time is needed, a narrow band filter of 705 ± 5 should be used to reduce the illumination intensity. Using narrow band filters would also help to reduce dye bleaching and vibration noise.

As an example we suggest narrow band filters for measuring spontaneous epileptiform events in cortical slices. Epileptiform events have large signals (Tsau et al., 1998b, 1999) so that using a narrow band filter can help to increase total recording time and reduce vibration noise.

3.6. Comparing NK3630 with the fluorescent dye RH795

In the course of voltage-sensitive dye development, fluorescence and absorption dyes have been more or less equally developed (reviewed by Ebner and Chen, 1995). Absorption dyes usually need trans-illumination, which is inconvenient or impossible for in vivo measurements [one exception is that in turtle visual cortex, a transillumination arrangement and absorption dye

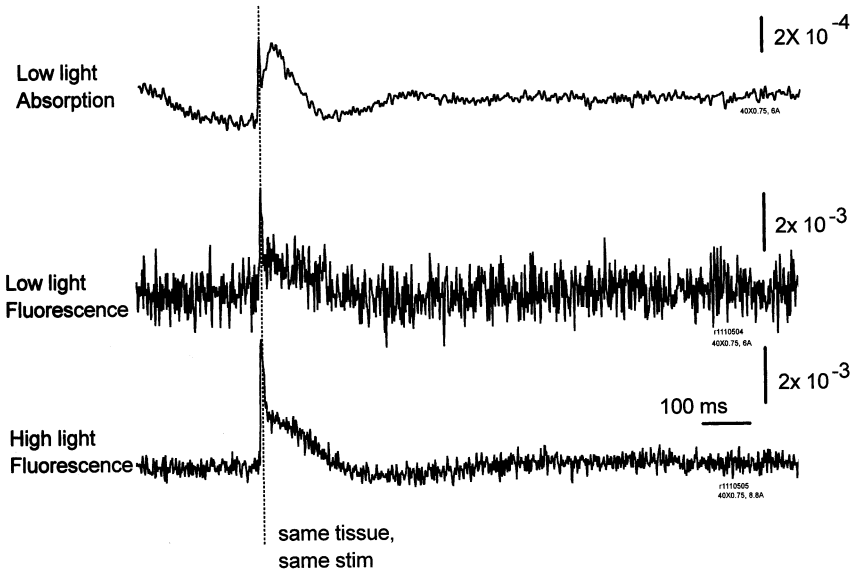

Fig. 8. Fluorescence and absorption signals from the same cortical tissue. The slice was stained by NK3630 (0.02 mg/ml) and RH795 (0.1 mg/ml) simultaneously. The two kinds of optical signals were recorded by a 40 × (0.75 N.A) water immersion objective from the same area (40×40 μm^2) in layer II–III of the somatosensory cortex. The stimulus electrode was placed in the deep layers in beam of the recording area. The stimulus intensity was 30% of the intensity that yields the maximum response. The signals were digitally filtered between 2 and 300 Hz. Top two traces: at a low illumination intensity (1.6×10^{11} photons per ms, 100 W halogen filament lamp running at 6 A), absorption measurement has a better signal-to-noise ratio. Bottom trace: at a high illumination intensity ($\sim 10^{12}$ photons per ms per mm^2, 100 W lamp running at 8.8 A), the signal-to-noise ratio for the fluorescence measurement improved significantly.

was used (Senseman and Robins, 1999)]. In brain slice both epi- and trans-illumination can be used, so whether the absorption or the fluorescent dyes are better remains an open question. In artificial membrane systems (Loew and Simpson, 1981; Fluhler et al., 1985) and cultured neuron systems (Chien and Pine, 1991; Stepnoski et al., 1991), fluorescent dyes have larger fractional changes ($dI/I = \sim 0.5$–5%) which are about 10–100 times larger than those of absorption dyes. In brain slices, however, this larger fractional change does not necessarily translate into higher signal-to-noise ratio. Cohen and Lesher (1986) have reasoned that in a tissue where a large fraction of dye molecules is bound to non-excitable membrane (connective tissue and glial membrane), absorption dyes could give a larger signal-to-noise ratio. In cortical tissue the ratio of excitable/nonexcitable membrane is unknown. In addition during many neuronal events only a small fraction of neurons are active (Wu et al., 1999b, 2001).

The use of absorption dyes in brain slices has been systematically evaluated; NK3630 (RH482) is one of the best absorption dyes and long-term optical recordings using this dye is possible (Momose-Sato et al., 1999). Meanwhile long-term optical recording using fluorescent dyes has also been demonstrated (Tominaga et al., 2000). However, exactly which kind of dye can have larger signal-to-noise ratio and longer total recording time has not been evaluated. Here we compared the signal-to-noise ratio of a popular fluorescent styryl dye RH795 to that of NK3630 under the same illumination intensity (slice receives a similar level of light exposure and total recording time).

The total recording time of RH795 seems to be limited by phototoxicity. When RH795 stained slices were illuminated with 520 nm light at an intensity of $\sim 10^{12}$ photons per ms per mm^2, in all three preparations tested LFP and optical signal disappeared in two to five trials of 2 min exposures. After the signals disappeared, the fluorescence of the stained tissue remained at $\sim 80\%$ of the pre-exposure level, suggesting that phototoxicity occurred but bleaching was insignificant.

At this level of illumination intensity, the signal-to-noise ratio for RH795 was about 6 for a 'fast' response evoked by a shock of 20% of saturation intensity ($n = 3$ slices).

For absorption measurement with NH3630, we adjusted the illumination intensity to obtain a signal-to-noise ratio of 6 (stimulated by a shock of 20% of saturation). The signal was only reduced to 50% after 40 min of exposure (two slices), which is about an order of magnitude longer than RH795. We think that regarding phototoxicity, absorption dye NK3630 is significantly better than fluorescent dye RH795 in brain slice experiments.

Fig. 8 compares the signal-to-noise ratio of a fluorescence measurement and absorption measurement from the same tissue under the same illumination intensity. The slice was stained with RH795 and NK3630 at the same time. Since the two dyes absorb different light

wavelengths, their signals remained unchanged when the tissue was stained with the other dye. This allowed us to evaluate the signal size of the same evoked activity in the same neuronal population. The fast response (Fig. 2B-1) had little trial-to-trial variation at the same stimulus intensity. We thus measured one trial with trans-illumination at 705 nm (absorption of NK3630), and then measured one trial again with the epi-illumination arrangement, illuminating the tissue with 520 nm light and measuring the signal in 610 nm and longer wavelengths (fluorescence of RH795). With the same illumination intensity (1.6×10^{11} photons per ms per mm^2) RLI for absorption measurement was 1.5×10^{10} photons per ms per mm^2 and the absorption signal for the same activity in the same tissue was $\sim 4 \times 10^{-4}$. The resting fluorescence intensity of the tissue was about 3×10^7 photons per ms per mm^2 and the fluorescence signal (dF/F) was $\sim 5 \times 10^{-3}$ (Fig. 8 middle trace). Although the fractional change of the fluorescent dye was about 10 times larger than that of the absorption dye, the signal-to-noise ratio for the fluorescence measurement was substantially lower (Fig. 8, top two traces). The signal-to-noise ratio of our fluorescence measurement was similar to the one measured from a hippocampal slice stained with another fluorescent dye, Di-4-ANEPPS (Tominaga et al., 2000). Increasing illumination intensity to 10^{12} photons per ms per mm^2 significantly increased the signal-to-noise ratio of the same evoked activity (Fig. 8 bottom trace), however, the total recording time at this level would be significantly shortened.

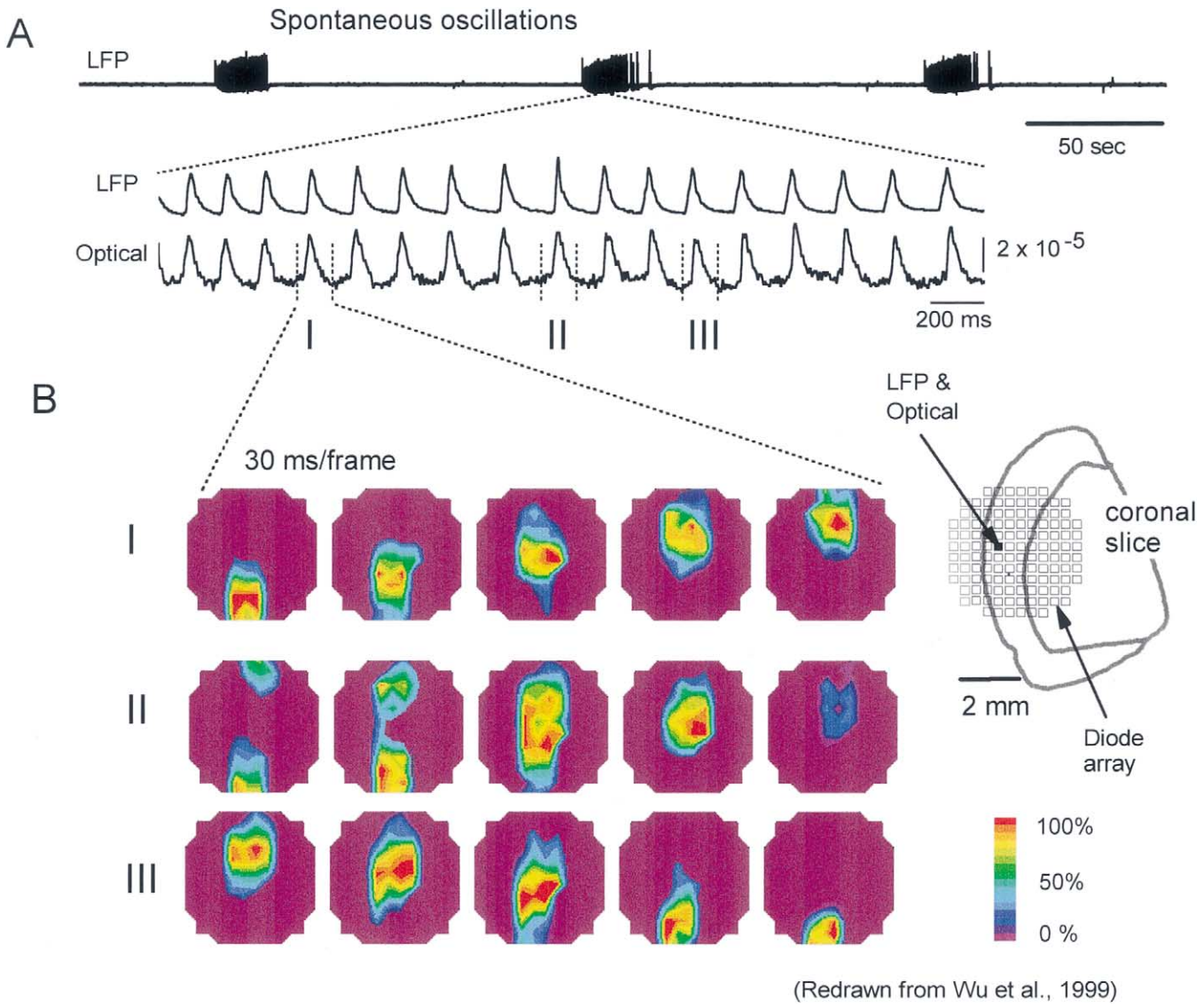

Fig. 9. Propagating activation during an oscillation. (A) A spontaneous oscillation occurred in the cortical slices bathed in low magnesium ACSF. Each episode started with an initial spike, and many cycles of oscillation followed. Three cycles, I, II and III, are shown in the pseudocolor images in B. (B) Imaging showed that these different cycles had different initiation sites and different propagation directions (redrawn from Wu et al., 1999b).

This direct comparison suggests that with a long total recording time, fluorescence measurements are only able to visualize large signals (e.g. from epileptiform activity or the fast response evoked by a strong electrical shock) in single trials. In contrast, absorption measurements are able to detect small and non-averageable activities (e.g. oscillations, Wu et al., 1999b; Fig. 9).

3.7. Application examples

The first example is to examine the spatiotemporal properties of a population oscillation (Wu et al., 1999b; Fig. 9). This activity is an 'epoch oscillation' which spontaneously occurs in cortical slices bathed in low magnesium ACSF. Each epoch started with an initial spike and was followed by many cycles of oscillations (Fig. 9A). In LFP recordings each oscillation cycle was similar (Fig. 9A) but imaging showed that different cycles (cycles I, II and III in Fig. 9B) initiated at different locations. In this example the oscillation could not be detected by CCD devices because the signal was small ($\sim 10^{-4}$) and averaging could not be applied to increase the signal-to-noise ratio.

Fig. 10 shows an example of mapping a special 'potentiation' in the amygdaloid. When the fiber track leading to the amygdaloid nuclei was stimulated at 1 Hz for 15 min, a slow potentiation occurred in different nuclei of the amygdaloid complex (Li et al., 1998). With voltage-sensitive dye imaging different degrees of potentiation in different clusters of neurons in amygdaloid complex could be examined simultaneously. Fig. 10 shows that one small cluster had more than 100 times stronger a potentiation than the neighboring areas. The cluster was only about 166 um wide and simultaneously imaging the whole area was much easier when identifying the potentiated region than using field potential or intracellular recordings. Without multi-location recording this study would be difficult. In the measurement shown in Fig. 10 the LFP electrode was only 300 um away from the locus with the large potentiation but

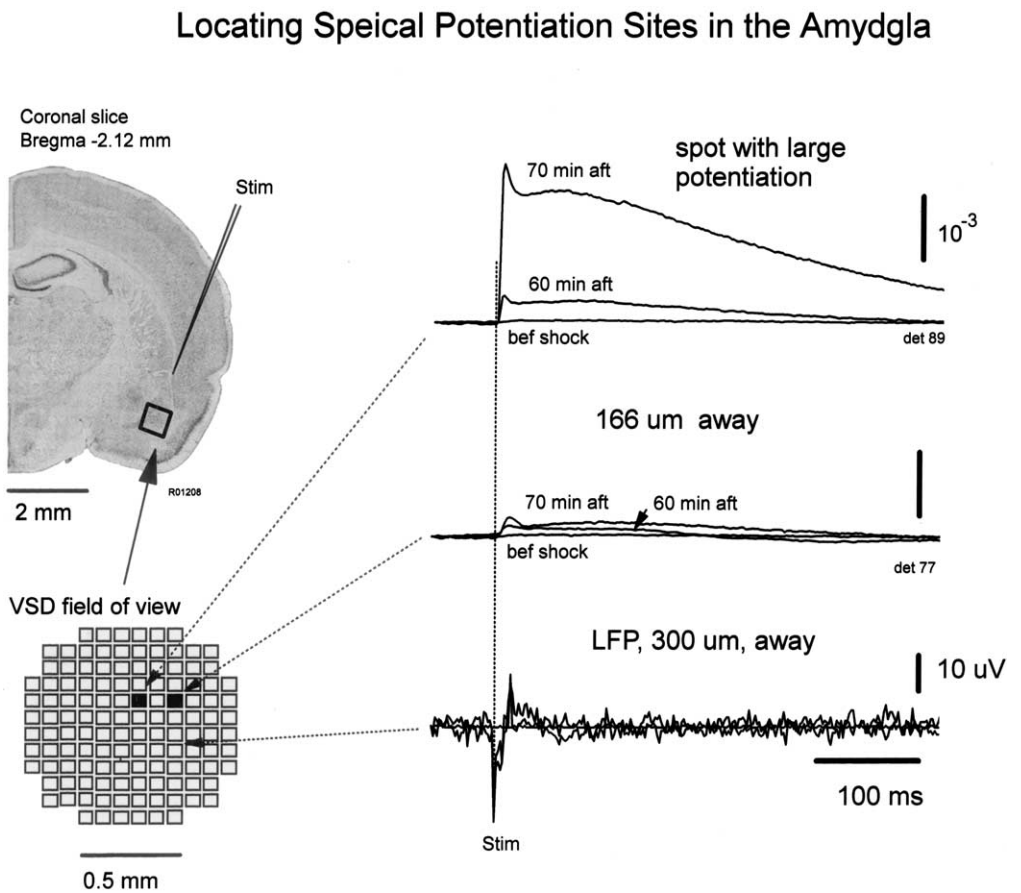

Fig. 10. A special potentiation in amygdaloid. The amygdaloid complex area, a box about 1×1 mm^2, was imaged by VSD imaging. A fast response was elicited by an electrical shock to the external capsule (right traces). A train of potentiation shocks at 1 Hz $\times$ 15 min was applied to the stimulation electrode. About 70 min after the potentiation shocks, one small area showed a much larger response, about 100 times larger than the response before the shocks (upper three traces on the right). This dramatic enhancement of evoked response only occurred under one detector (83×83 μm^2). Recordings 166 μm away from the site showed much less potentiation, and a LFP electrode 330 μm away from the site did not show any significant potentiation.

showed no potentiation at all (Fig. 10). VSD imaging provided a map of the large potentiation in the tissue. After the imaging the same tissue could be used for immunochemistry or in situ hybridization to study the subtypes of receptors in different neuron clusters which were responsible for this large potentiation.

4. Conclusion

Data in this report suggest that using the combination of absorption dyes, diode array and an advanced vibration control may achieve an optimum condition for measuring population activity in brain slices. With this combination about 500 locations in 1 mm^2 of cortical tissue can be measured simultaneously with a sensitivity comparable to that of LFP electrode.

Acknowledgements

We thank Dr Lawrence B. Cohen for critical and very helpful comments, Dr H. Li and Dr M.A. Rogawski for help with the amygdaloid slice experiment, and A. Schaefer and H. Frost for technical assistance with the experiments and manuscript preparation. Supported by NIH NS36477 and a Whitehall Foundation grant.

References

Albowitz B, Kuhnt U. Evoked changes of membrane potential in guinea pig sensory neocortical slices: an analysis with voltage-sensitive dyes and a fast optical recording method. Exp Brain Res 1993;93:213–25.

Antic S, Major G, Zecevic D. Fast optical recordings of membrane potential changes from dendrites of pyramidal neurons. J Neurophysiol 1999;82:1615–21.

Cacciatore TW, Brodfuehrer PD, Gonzalez JE, Jiang T, Adams SR, Tsien RY, Kristan WB, Kleinfeld D. Identification of neural circuits by imaging coherent electrical activity with FRET-based dyes. Neuron 1999;23:449–59.

Chien CB, Pine J. Voltage-sensitive dye recording of action potentials and synaptic potentials from sympathetic microcultures. Biophys J 1991;60:697–711.

Cohen LB, Salzberg BM. Optical measurement of membrane potential. Rev Physiol Biochem Pharmacol 1978;83:35–88.

Cohen LB, Lesher S. Optical monitoring of membrane potential: methods of multisite optical measurement. Soc Gen Physiol Ser 1986;40:71–99.

Cohen LB, Keynes RD, Hille B. Light scattering and birefringence changes during nerve activity. Nature 1968;218:438–41.

Colom LV, Saggau P. Spontaneous interictal-like activity originates in multiple areas of the CA2–CA3 region of hippocampal slices. J Neurophysiol 1994;71:1574–85.

Demir R, Haberly LB, Jackson MB. Sustained and accelerating activity at two discrete sites generate epileptiform discharges in slices of piriform cortex. J Neurosci 1999;19:1294–306.

Demir R, Haberly LB, Jackson MB. Characteristics of plateau activity during the latent period prior to epileptiform discharges in slices from rat piriform cortex. J Neurophysiol 2000;83:1088–98.

Ebner TJ, Chen G. Use of voltage-sensitive dyes and optical recordings in the central nervous system. Prog Neurobiol 1995;46:463–506.

Fluhler E, Burnham VG, Loew LM. Spectra membrane binding, and potentiometric responses of new charge shift probes. Biochemistry 1985;24:5749–55.

Grinvald A, Hildesheim R, Farber IC, Anglister L. Improved fluorescent probes for the measurement of rapid changes in membrane potential. Biophys J 1982a;39:301–8.

Grinvald A, Manker A, Segal M. Visualization of the spread of electrical activity in rat hippocampal slices by voltage-sensitive optical probes. J Physiol 1982b;333:269–91.

Gupta RK, Salzberg BM, Grinvald A, Cohen LB, Kamino K, Lesher S, Boyle MB, Waggoner AS, Wang CH. Improvements in optical methods for measuring rapid changes in membrane potential. J Membr Biol 1981;58:123–37.

Hirota A, Sato K, Momose-Sato Y, Sakai T, Kamino K. A new simultaneous 1020-site optical recording system for monitoring neural activity using voltage-sensitive dyes. J Neurosci Methods 1995;56:187–94.

Kojima S, Nakamura T, Nidaira T, Nakamura K, Ooashi N, Ito E, Watase K, Tanaka K, Wada K, Kudo Y, Miyakawa H. Optical detection of synaptically induced glutamate transport in hippocampal slices. J Neurosci 1999;19:2580–8.

Laaris N, Carlson GC, Keller A. Thalamic-evoked synaptic interactions in barrel cortex revealed by optical imaging. J Neurosci 2000;20:1529–37.

Li H, Weiss SRB, Chuang D, Post RM, Rogawski MA. Bidirectional synaptic plasticity in the rat basolateral amygdala: characterization of an activity-dependent switch sensitive to the presynaptic metabotropic glutamate receptor antagonist 2S-ethylglutamic acid. J Neurosci 1998;18:1662–70.

Loew LM, Simpson LL. Charge-shift probes of membrane potential: a probable electrochromic mechanism for *p*-aminostyrylpyridinium probes on a hemispherical lipid bilayer. Biophys J 1981;34:353–65.

Loew LM, Cohen LB, Dix J, Fluhler EN, Montana V, Salama G, Wu J-Y. A naphthyl analog of the aminostyryl pyridinium class of potentiometric membrane dyes shows consistent sensitivity in a variety of tissue, cell, and model membrane preparations. J Membr Biol 1992;130:1–10.

Momose-Sato Y, Sato K, Arai Y, Yazawa I, Mochida H, Kamino K. Evaluation of voltage-sensitive dyes for long-term recording of neural activity in the hippocampus. J Membr Biol 1999;172:145–57.

Pazdalski PS, Tsau Y, Wu J-Y. Light scattering in cortical tissue as an indicator of normal and epileptiform activity: an in vitro study. Neurosci Abstr 1998;24:1059.

Ross W, Salzberg B, Cohen L, Grinvald A, Davila H, Waggoner A, Wang C. Changes in absorption, fluorescence, dichroism, and birefringence in stained giant axons: optical measurement of membrane potential. J Membr Biol 1977;33:141–83.

Senseman DM, Robins KA. Modal behavior of cortical neural networks during visual processing. J Neurosci 1999;19(RC3):1–7.

Senseman DM, Vasquez S, Nash PL. Animated pseudocolor activity maps PAMs: scientific visualization of brain electrical activity. In: Schilds D, editor. Information Processing of Chemical Sensory Stimuli in Biological and Artificial Systems, NATO ASI Series, vol. H39. Berlin: Springer, 1999:329–47.

Shoham D, Glaser DE, Arieli A, Kenet T, Wijnbergen C, Toledo Y, Hildesheim R, Grinvald A. Imaging cortical dynamics at high spatial and temporal resolution with novel blue voltage-sensitive dyes. Neuron 1999;24:791–802.

Stepnoski RA, La Porta A, Raccuia-Behling F, Blonder GE, Slusher RE, Kleinfeld D. Noninvasive detection of changes in membrane potential in cultured neurons by light scattering. Proc Natl Acad Sci USA 1991;88:9382–6.

Tanifuji M, Sugiyama T, Murase K. Horizontal propagation of excitation in rat visual cortical slices revealed by optical imaging. Science 1994;266:1057–9.

Tasaki I, Watanabe A, Carnay L. Changes in fluorescence, turbidity, and bireference associated with nerve excitation. Proc Natl Acad Sci USA 1968;61:883–8.

Taylor AL, Cacciatore TW, Gonzalez JE, Rao J, Cottrell GW, Tsien RY, Kleinfeld D, Kristan WBJ. Improved FRET-based voltage sensitive dye imaging in leech. Neurosci Abstr 2000;26:1722.

Tominaga T, Tominaga Y, Yamada H, Matsumoto G, Ichikawa M. Quantification of optical signals with electrophysiological signals in neural activities of Di-4-ANEPPS stained rat hippocampal slices. J Neurosci Methods 2000;102:11–23.

Tsau Y, Guan L, Wu J-Y. Initiation of spontaneous epileptiform activity in the neocortical slice. J Neurophysiol 1998a;80:978–82.

Tsau Y, Guan L, Wu J-Y. Initiation of spontaneous epileptiform events in neocortical slices: dominant focus. Neurosci Abstr 1998b;24:2141.

Tsau Y, Guan L, Wu J-Y. Epileptiform activity can be initiated in various neocortical layers: an optical imaging study. J Neurophysiol 1999;82:1965–73.

Wu J-Y, Cohen LB. Fast multisite optical measurement of membrane potential. In: Biological Techniques: Fluorescent and Luminescent Probes for Biological Activity. New York: W.T. Mason, Academic Press, 1993:389–404.

Wu J-Y, Cohen LB, Falk CX. Fast Multisite Optical Measurement of Membrane Potential. With Two Examples. Fluorescent and Luminescent Probes for Biological Activity. W.T. Mason, Academic Press, 1999a:222–38.

Wu J-Y, Guan L, Tsau Y. Propagating activation during oscillations and evoked responses in neocortical slices. J Neurosci 1999b;19:5005–15.

Wu J-Y, Guan L, Bai L, Yang Q. Spatiotemporal properties of an evoked population activity in rat sensory cortical slices. J Neurophysiol 2001;86:2461–74.

Zecevic D. Multiple spike-initiation zones in single neurons revealed by voltage-sensitive dyes. Nature 1996;381:322–5.